Pré-Publicações do Departamento de Matemática
Universidade de Coimbra
Preprint Number 06–03

HIGH ORDER METHODS AND NUMERICAL BOUNDARY CONDITIONS

ERCÍLIA SOUSA

Abstract: In this paper we present high-order difference schemes for convection diffusion problems. When we apply high order numerical methods to problems where physical boundary conditions are not periodic there is a need to choose adequate numerical boundary conditions in order to preserve the high-order accuracy. Next to the boundary we do not usually have enough discrete points to apply the high-order scheme and therefore at these nodes we must consider different approximations, named the numerical boundary conditions.

The choice of numerical boundary conditions can influence the overall accuracy of the scheme and most of the times do influence the stability. Here, we discuss which orders of accuracy are reasonable to be considered at the numerical boundary conditions, such that we do not pay a high price in accuracy and stability.

Keywords: high-order finite differences, convection–diffusion, boundary conditions.

1. Introduction

In order to compute approximate solutions for evolutionary partial differential equations with either explicit or implicit schemes, it is necessary to use some form of local approximation; local in the sense that solution values at local nodes are used to generate an approximate solution value at a new time level. In finite differences it is usual to try to make the local domain as compact as possible, for instance using only adjacent nodes when updating at a node. The domain of local approximation may need to be large because the degree of the equation is high or it may need to be enlarged to accommodate a higher order local approximation for a low order differential equation. In either case schemes are usually derived for infinite space domains; when space boundaries occur they prevent such high order schemes from being applied directly. One method to deal with the second of these situations, a high order local approximation to a low order equation, is simply to use a lower order scheme immediately near boundaries and use a high order scheme for the major part of the interior of the domain. Whether this is useful will

Received February 1, 2006.

depend on the nature of the problem being approximated. If interest is centered on dynamics in the interior and on time scales where boundary effects have not propagated to the region of interest, then this will be a reasonable approximation. If the boundary influences the interior quickly, little may be gained by using a high order scheme to accurately propagate low order errors from the boundaries to the interior.

In the majority of cases, to provide a modified scheme at a boundary which retains the accuracy of the scheme used in the interior of the domain will be very difficult.

Here, we analyse a class of high-order schemes, for the convection-diffusion equation and discuss which orders of accuracy are reasonable to be considered at the numerical boundary conditions so that, it will still be worthwhile to use an higher-order scheme in the interior.

Finite difference schemes typically consist of replacement of the individual derivative terms in the partial differential equation by a set of discretised approximations (see e.g. Smith [1]). However, different techniques have been suggested for deriving finite differences for the unsteady convection-diffusion equation (see e.g. Kolesnikov and Baker [2], Morton and Sobey [3] and Xu *et al* [4]).

Morton and Sobey [3], derived the Lax-Wendroff scheme, due to Lax and Wendroff [5], and the Quickest scheme, due to Leonard [6], using an evolution operator. In this paper we derive high-order schemes using the evolution operator, associated to the convection-diffusion problem, considered in Morton and Sobey [3].

2. High-order schemes

Consider the one-dimensional problem with constant velocity V in the positive x direction and constant diffusion with coefficient $D > 0$:

$$\frac{\partial u}{\partial t} + V\frac{\partial u}{\partial x} = D\frac{\partial^2 u}{\partial x^2}, \quad t > 0, \quad x \in \mathbb{R}, \tag{1}$$

subject to the initial condition

$$u(x,0) = u_0(x) \tag{2}$$

and the boundary condition

$$u(x,t) = 0 \quad \text{as} \quad |x| \to \infty. \tag{3}$$

This initial value problem can be solved in closed form using Fourier transforms in x to obtain the exact solution,

$$u(x,t) = \frac{1}{\sqrt{\pi}} \int_{-\infty}^{+\infty} u_0(x - Vt + 2\sqrt{Dt}\xi)\mathrm{e}^{-\xi^2} d\xi. \tag{4}$$

Let us choose a uniform time step Δt. Applying the result to evolution over one time step, from time t_n to $t_{n+1} = t_n + \Delta t$ write

$$u(x, t_n + \Delta t) = \int_{-\infty}^{+\infty} u(\eta, t_n) G(x - \eta; \Delta t) d\eta,$$

where the Green's function is given by

$$G(z;\tau) = \frac{1}{\sqrt{D\pi\tau}} \mathrm{e}^{-(z-V\tau)^2/4D\tau}.$$

As showed by Morton and Sobey [3] to derive either finite difference or finite element approximations we substitute an approximation to $u(\eta, t_n)$ in this integral, and exploit the fact that the integration of a global polynomial can be carried out exactly.

2.1. Finite difference schemes. Suppose we have approximations U_j^n to the values $u(x_j, t_n)$ at the mesh points

$$x_j = j\Delta x, \quad j = 0, \pm 1, \pm 2, \ldots,$$

where Δx denotes the uniform space step. For this set of values we denote $\mathbf{U}^n := \{U_j^n\}$ and $p_j(x; \mathbf{U}^n)$ the interpolating polynomial, associated with the points x_j, through U_j^n and the values at a certain number of neighboring points. Then finite difference schemes can be generated from evolution of this interpolating approximation by

$$U_j^{n+1} = \int_{-\infty}^{+\infty} p_j(\eta; \mathbf{U}^n) G(x_j - \eta; \Delta t) d\eta. \tag{5}$$

If the approximation scheme obtained comes from approximating $\mathbf{U}^n$ near x_j by a polynomial $p_j(x; \mathbf{U}^n)$, of degree R,

$$p_j(x; \mathbf{U}^n) = \sum_{r=0}^{R} b_{jr}(x - x_j)^r,$$

then

$$U_j^{n+1} = \frac{1}{\sqrt{\pi}} \int_{-\infty}^{+\infty} p_j(x - V\Delta t + 2\sqrt{D\Delta t}\xi; \mathbf{U}^n) \mathrm{e}^{-\xi^2} d\xi.$$

When evaluating the previous integral we come across integrals of the form

$$a_r = \frac{1}{\sqrt{\pi}} \int_{-\infty}^{+\infty} \xi^r \mathrm{e}^{-\xi^2} d\xi. \tag{6}$$

For $r = 0, 1, 2, \ldots$ the values of the integrals can be obtained using the recurrence relation

$$a_0 = 1, \quad a_1 = 0$$

$$a_r = \frac{1}{2}(r-1)a_{r-2}, \quad r = 2, \ldots.$$

The approximate solution can be written as

$$\begin{aligned} U_j^{n+1} &= \frac{1}{\sqrt{\pi}} \int_{-\infty}^{+\infty} \sum_{r=0}^{R} b_{jr}(-V\Delta t + 2\sqrt{D\Delta t}\xi)^r \mathrm{e}^{-\xi^2} d\xi \\ &= \sum_{r=0}^{R} b_{jr} \frac{1}{\sqrt{\pi}} \int_{-\infty}^{+\infty} \sum_{n=0}^{r} \binom{r}{n} (-V\Delta t)^{r-n} (2\sqrt{D\Delta t})^n \xi^n \mathrm{e}^{-\xi^2} d\xi \\ &= \sum_{r=0}^{R} b_{jr} \sum_{n=0}^{r} \binom{r}{n} (-V\Delta t)^{r-n} (2\sqrt{D\Delta t})^n a_n, \end{aligned}$$

where a_n is defined by (6). We have,

$$\begin{aligned} U_j^{n+1} &= b_{j0} - b_{j1}V\Delta t + b_{j2}[V^2(\Delta t)^2 + 2D\Delta t] - b_{j3}[V^3(\Delta t)^3 + 6VD(\Delta t)^2] \\ &\quad + b_{j4}[V^4(\Delta t)^4 + 12V^2D(\Delta t)^3 + 12D^2(\Delta t)^2] \\ &\quad - b_{j5}[V^5(\Delta t)^5 + 20V^3(\Delta t)^3 D\Delta t + 60V\Delta t D^2(\Delta t)^2] + \ldots. \end{aligned}$$

Within this framework one can obtain different high-order schemes by different interpolations on a uniform mesh. We use the usual central, backward, forward, second difference and fourth difference operators,

$$\Delta_0 U_j := \frac{1}{2}(U_{j+1} - U_{j-1}), \quad \Delta_- U_j := U_j - U_{j-1}, \quad \Delta_+ U_j := U_j - U_{j-1}$$

$$\delta^2 U_j := U_{j+1} - 2U_j + U_{j-1}, \quad \text{and} \quad \delta^4 U_j := U_{j+2} - 4U_{j+1} + 6U_j - 4U_{j-1} + U_{j-2}$$

to evaluate the coefficients b_{jr} in terms of the nodal values $\mathbf{U}^n$ and obtain high-order schemes.

For the uniform space step Δx and time step Δt let:

$$\mu = \frac{D\Delta t}{(\Delta x)^2}, \quad \nu = \frac{V\Delta t}{\Delta x};$$

ν is the Courant (CFL) number.

Quadratic interpolation: If we interpolate U_{j-1}, U_j and U_{j+1} , then

$$U_j^{n+1} = \{1 - \nu\Delta_0 + (\frac{1}{2}\nu^2 + \mu)\delta^2\}U_j^n. \tag{7}$$

Cubic interpolation: If we extend $p_j(x, \mathbf{U}^n)$ to include a cubic term, that is, using U_{j-2} as well as U_{j-1}, U_j and U_{j+1}, then

$$U_j^{n+1} = \{1 - \nu\Delta_0 + (\frac{1}{2}\nu^2 + \mu)\delta^2 + \frac{1}{6}\nu(1 - \nu^2 - 6\mu)\delta^2\Delta_-\}U_j^n. \tag{8}$$

Quartic interpolation: If a quartic interpolant of $U_{j-2}, \ldots, U_{j+2}$ is used then the approximation formula for U_j^{n+1} becomes

$$\begin{aligned} U_j^{n+1} &= \{1 - \nu\Delta_0 + (\frac{1}{2}\nu^2 + \mu)\delta^2 + \frac{1}{6}\nu(1 - \nu^2 - 6\mu)\delta^2\Delta_- \\ &\quad + \frac{1}{24}[12\mu^2 - 2\mu - 12\mu\nu(1-\nu) + \nu(1-\nu^2)(2-\nu)]\delta^4\}U_j^n. \end{aligned} \tag{9}$$

Quintic approximation: If a quintic interpolant of $U_{j-3}, \ldots, U_{j+2}$ is used then the approximation formula for U_j^{n+1} becomes

$$\begin{aligned} U_j^{n+1} &= \{1 - \nu\Delta_0 + (\frac{1}{2}\nu^2 + \mu)\delta^2 + \frac{1}{6}\nu(1 - \nu^2 - 6\mu)\delta^2\Delta_- \\ &\quad + \frac{1}{24}[12\mu^2 - 2\mu - 12\mu\nu(1-\nu) + \nu(1-\nu^2)(2-\nu)]\delta^4 \\ &\quad + \frac{1}{120}[-4\nu + 5(\nu^3 + 6\nu\mu) - (\nu^5 + 20\nu^3\mu + 60\nu\mu^2)]\delta^4\Delta_-\}U_j^n. \end{aligned} \tag{10}$$

Note that the quadratic interpolation and the cubic interpolation are respectively the well known Lax-Wendroff scheme [5] and Quickest scheme [6]. The schemes not yet studied in the literature are those obtained by the quartic interpolation (9) and quintic interpolation (10).

2.2. Global error and truncation error. The schemes in the previous section can be written in the matricial form,

$$\mathbf{U}^{n+1} = A\mathbf{U}^n, \tag{11}$$

where the matrix A contains the coefficients of the difference formulas. In order to have a matrix of finite dimensions we assume that the boundary conditions are periodic.

For the exact solution, we denote $\mathbf{u}^n$ the set $\mathbf{u}^n := \{u(x_j, t_n)\}$. The error $E^n = \mathbf{u}^n - \mathbf{U}^n$ for the set of nodal errors, is given by

$$E^{n+1} = AE^n + \Delta t T^n, \tag{12}$$

where T^n is the truncation error. For any chosen norm for the error, the practical stability requirement is that $||A|| \leq 1$. Then a global error bound is given by

$$||E^n|| \leq ||E^0|| + \Delta t \sum_{j=0}^{n-1} ||T^j|| \leq ||E^0|| + (n\Delta t) \max_{0 \leq j \leq n-1} ||T^j||.$$

Since we assume the boundary conditions are periodic, the stability conditions obtained by $||A||_2 \leq 1$, where $||\cdot||_2$ is the 2-norm, are equivalent to the stability conditions obtained using the von Neumann Fourier analysis [7].

The following local truncation error of the schemes can be derived using the modified equation method as in Warming and Hyett [8] or the Peano kernel theorem as in Morton and Sobey [3].

Quadratic interpolation: (Lax-Wendroff)

$$\begin{aligned} \Delta t T_j^n &= \frac{1}{6}\Delta x^3 \nu(1-\nu^2-6\mu) U_{x^3}^n(x_j) \\ &+ \frac{1}{24}\Delta x^4 (12\mu^2 - 2\mu + 3\nu^2(1-\nu^2-4\mu)) U_{x^4}^n(x_j) + \ldots \end{aligned} \tag{13}$$

Cubic interpolation: (Quickest)

$$\Delta t T_j^n = \frac{1}{24}\Delta x^4 (12\mu^2 - 2\mu - 12\mu\nu(1-\nu) + \nu(1-\nu^2)(2-\nu)) U_{x^4}^n(x_j) + \ldots$$

Quartic interpolation: We have,

$$\begin{aligned} \Delta t T_{|x_j} &= \frac{1}{120}\Delta x^5 \left(-4\nu + 5(\nu^3 + 6\nu\mu) - (\nu^5 + 20\nu^3\mu + 60\nu\mu^2)\right) U_{x^5}^n \\ &+ \ldots \end{aligned} \tag{14}$$

Quintic interpolation: We have,

$$\begin{aligned} \Delta t T_{|x_j} &= \frac{1}{720}\Delta x^6 \left(-12\nu + 4(\nu^2 + 2\mu) + 15(\nu^3 + 6\nu\mu) - 5(\nu^4 + 12\nu^2\mu + 12\mu^2)\right. \\ &\left. -3(\nu^5 + 20\nu^3\mu + 60\nu\mu^2) + (\nu^6 + 30\nu^4\mu + 120\mu^3 + 180\mu^2\nu^2)\right) U_{x^6}^n + \ldots \end{aligned}$$

On theoretical grounds, over a finite interval of time these estimates are sensitive to the values of ν and μ considered, since μ and ν need not be constant and may vary depending on how Δx and Δt are related when we refine the mesh. Nevertheless, in general, we expect the quadratic interpolation to be close to $O(\Delta x^2)$, the cubic interpolation close to $O(\Delta x^3)$, the quartic interpolation close to $O(\Delta x^4)$ and the quintic interpolation should be $O(\Delta x^5)$.

2.3. Fourier stability analysis. Clearly the von Neumann condition is very important both practically and theoretically. Even for variable coefficient problems it can be applied locally (with local values of the coefficients) and because instability is a local phenomenon, due to the high frequency modes being the most unstable, it gives necessary stability conditions which can often be shown to be sufficient.

The following important points should be noted concerning the von Neumann method of examining stability. The method which is based on Fourier analysis applies only if the coefficients of the linear difference equation are constant. Boundary conditions are neglected by the von Neumann method which applies in theory only to pure initial value problems with periodic initial data. It does however provide necessary conditions for stability of constant coefficient problems regardless of type of boundary conditions.

If we assume periodic boundary conditions the von Neumann analysis is based on the decomposition of the numerical solution into a Fourier series as

$$U_j^n = \sum_{p=-N}^{N} \kappa_p^n \mathrm{e}^{\mathrm{i}\xi_p (j\Delta x)}$$

where $\mathrm{i} = \sqrt{-1}$, κ_p^n is the amplification factor of the p-th harmonic and $\xi_p = \dfrac{p\pi}{N\Delta x}$. The product $\xi_p \Delta x$ is often called the phase angle:

$$\theta = \xi_p \Delta x$$

and covers the domain $(-\pi, \pi)$ in steps of π/N. The region around $\theta = 0$ corresponds to the low frequencies while the region $\theta = \pi$ is associated with the high-frequencies. In particular, the value $\theta = \pi$ corresponds to the highest frequency resolvable on the mesh, namely the frequency of wavelength $2\Delta x$.

Considering a single mode, $\kappa^n e^{ij\theta}$, its time evolution is determined by the same numerical scheme as the complete numerical solution U_j^n. Hence inserting a representation of this form into a numerical scheme we obtain a stability condition by getting an upper bound for the amplification factor, κ.

The amplification factor is said to satisfy the *von Neumann condition* if there is a constant K such that

$$|\kappa(\xi)| \leq 1 + K\Delta t, \quad \forall \xi \in \mathbb{R}. \tag{15}$$

However, for some problems the presence of the arbitrary constant in (15) is too generous for practical purposes, although being adequate for eventual convergence in the limit $\Delta t \to 0$. In practice, the inequality (15) is substituted by the following stronger condition

$$|\kappa(\xi)| \leq 1, \quad \forall \xi \in \mathbb{R}. \tag{16}$$

This has been called practical stability by Richtmyer and Morton [9] or strict stability by other authors. In some cases condition (15) allows numerical modes to grow exponentially in time for finite values of Δt. Therefore, the practical, or strict, stability condition (16) is recommended in order to prevent numerical modes from growing faster than the physical modes of the differential equation.

Next, we present some results on stability based in the von Neumann analysis for the four schemes.

The result that follows, about the Lax-Wendroff scheme, can be found in various works such as Warming and Hyett [8].

Proposition 1. *A necessary and sufficient condition for stability of the Lax-Wendroff scheme (the quadratic interpolation) is*

$$\nu^2 + 2\mu \leq 1.$$

The Quickest scheme is more complex than the Lax-Wendroff scheme and consequently so is its von Neumann stability analysis. A necessary stability condition for the Quickest scheme was given by Leonard [6]. In the next lemma we combine this necessary condition with an additional one.

Lemma 2. *If the Quickest scheme (cubic interpolation) is stable then*

$$\nu^2 + 6\mu\frac{1-2\nu}{3-2\nu} \leq 1, \qquad \nu^2 + 6\mu(1-2\nu) \geq -2\nu. \tag{17}$$

Proof: The amplification factor for the Quickest scheme is given by:

$$\begin{aligned}\kappa(\theta) &= 1 - \mathrm{i}\nu\sin\theta - (\nu^2+2\mu)(1-\cos\theta)\\ &\quad -\frac{\nu}{3}(1-\nu^2-6\mu)(1-\mathrm{e}^{-\mathrm{i}\theta})(1-\cos\theta).\end{aligned}$$

The necessary conditions (17) are obtained imposing $|\kappa(\pi)| \le 1$ since for $\theta = \pi$ we have the fundamental frequency that corresponds to the maximum wavelength. The necessary condition given by Leonard [6], the first condition of (17), was obtained from $\kappa(\pi) \ge -1$. We have

$$\kappa(\pi) = 1 - 2(\nu^2+2\mu) - \frac{4\nu}{3}(1-\nu^2-6\mu)$$

and if $|\kappa(\pi)| \le 1$ then

$$\nu^2 + 2\mu + \frac{2\nu}{3}(1-\nu^2-6\mu) \le 1 \qquad \nu^2 + 2\mu + \frac{2\nu}{3}(1-\nu^2-6\mu) \ge 0.$$

The conditions of the lemma follow from these inequalities. □

Although analytical von Neumann necessary and sufficient stability conditions have not been so far stated in the literature for the Quickest scheme, they have been computed numerically and plotted in papers by Leonard [6] and Morton and Sobey [3]. In the following theorem however we provide the analytical necessary and sufficient conditions for the Quickest scheme.

Theorem 3. *Let* $\alpha = 2\nu\mu - (\nu/3)(1-\nu^2)$, $n = (2\mu+\nu^2)^2 - \nu^2 + 2\alpha(1-2\nu)$ *and* $d = 4\alpha(2\mu+\nu^2-\nu-\alpha)$. *The Quickest scheme is stable if and only if*
(a) The condition $-2\mu + n - d \le 0$ *is satisfied;*
(b) Let $S = \{(\mu,\nu) : 0 \le n/2d \le 1\}$ *. For* $(\mu,\nu) \in S$ *,* $n^2/4d \le 2\mu$.

Proof: Considering the fact that

$$1-\cos\theta = 2\sin^2(\theta/2) \quad \text{and} \quad \sin^2\theta = 4\sin^2(\theta/2)(1-\sin^2(\theta/2)),$$

the modulus of the amplification factor of the Quickest scheme is given by

$$\begin{aligned}|\kappa(\theta)|^2 &= 1 - 8\mu\sin^2(\theta/2) + 4[(2\mu+\nu^2)^2 - \nu^2 + 2\alpha(1-2\nu)]\sin^4(\theta/2)\\ &\quad -16\alpha(2\mu+\nu^2-\nu-\alpha)\sin^6(\theta/2).\end{aligned}$$

Let $s = \sin^2(\theta/2)$ then

$$|\kappa(\theta)|^2 = 1 - 8\mu s + 4[(2\mu+\nu^2)^2 - \nu^2 + 2\alpha(1-2\nu)]s^2 - 16\alpha(2\mu+\nu^2-\nu-\alpha)s^3.$$

It follows $|\kappa(\theta)|^2 = 1 + 4s\phi(s)$, where for $s \in [0,1]$,

$$\phi(s) = -2\mu + [(2\mu+\nu^2)^2 - \nu^2 + 2\alpha(1-2\nu)]s - 4\alpha(2\mu+\nu^2-\nu-\alpha)s^2.$$

The stability condition $|\kappa(\theta)| \leq 1, \forall\theta \in \mathbb{R}$, is satisfied if and only if the condition

$$\phi(s) \leq 0, \quad s \in [0,1]$$

is satisfied. To prove this condition it is necessary and sufficient to prove that $\phi(0) \leq 0$, $\phi(1) \leq 0$ and that for $s_* \in [0,1]$ such that $\phi'(s_*) = 0$ then $\phi(s_*) \leq 0$.

We have that $\phi(0) = -2\mu$ and it is negative for all μ. The inequality $\phi(1) \leq 0$ is true if and only if the condition (a) of the theorem is satisfied. The zero of the function $\phi'(s)$ is

$$s_* = \frac{(2\mu+\nu^2)^2 - \nu^2 + 2\alpha(1-2\nu)}{8\alpha(2\mu+\nu^2-\nu-\alpha)}. \tag{18}$$

We want to find μ and ν such that $0 \leq s_* \leq 1$ and $\phi(s_*) \leq 0$. We have

$$\phi(s_*) = -2\mu + \frac{1}{4}\frac{[(2\mu+\nu^2)^2 - \nu^2 + 2\alpha(1-2\nu)]^2}{4\alpha(2\mu+\nu^2-\nu-\alpha)}. \tag{19}$$

The condition $\phi(s_*) \leq 0$ is verified if and only if

$$\frac{[(2\mu+\nu^2)^2 - \nu^2 + 2\alpha(1-2\nu)]^2}{16\alpha(2\mu+\nu^2-\nu-\alpha)} \leq 2\mu.$$

and this proves the theorem. □

We illustrate the stability conditions for the Lax-Wendroff scheme and Quickest scheme in Figure 1.

Although the analytical necessary and sufficient conditions presented above, for the Quickest scheme have a cumbersome form, we can check for a fixed value of ν or μ for which values the method is stable. For instance, if $\nu = 1/2$ and we want to find for which values of μ the method is practically stable, we have $\alpha = \mu - 1/8$, $n = 4(\mu-1/8)(\mu-3/8)$ and $d = 4(\mu-1/8)^2$. The first condition of the theorem is satisfied for all μ, but the second condition gives us that the method is practically stable for $0 \leq \mu \leq 9/8$. Similarly, if $\mu = 0$, then we easily can check that the conditions of the theorem give us $0 \leq \nu \leq 1$. Also, for $\nu = 0, 1$ we have that the method is stable for $\mu \leq 1/2$.

All the values obtained by these examples are in agreement with Figure 1, which was computed numerically.

Now, let us give necessary stability conditions for the schemes obtained by the quartic and quintic interpolations, that we call respectively, the quartic scheme and the quintic scheme.

Proposition 4. *(a) If the Quartic scheme is stable then*

$$0 \leq 2\alpha_2 + 4\alpha_3 - 8\alpha_4 \leq 1,$$

where $\alpha_2 = (\nu^2 + 2\mu)/2, \quad \alpha_3 = \nu(1-\nu-6\mu)/6$
and $\alpha_4 = (12\mu^2 - 2\mu - 12\mu\nu(1-\nu) + \nu(1-\nu^2)(2-\nu))/24.$
(b) If the Quintic scheme is stable then

$$0 \leq 2\alpha_2 + 4\alpha_3 - 8\alpha_4 - 15\alpha_5 \leq 1,$$

where $\alpha_5 = [-4\nu + 5(\nu^3 + 6\nu\mu) - (\nu^5 + 20\nu^3\mu + 60\nu\mu^2)]/120.$

Proof: Let $\theta = \xi\Delta x$. The amplification factor is given by

$$\begin{aligned}\kappa(\theta) &= 1 - \alpha_1(\mathrm{e}^{i\theta} - \mathrm{e}^{-i\theta}) + \alpha_2(\mathrm{e}^{i\theta} - 2 + \mathrm{e}^{-i\theta}) + \alpha_3(\mathrm{e}^{i\theta} - 3 + 3\mathrm{e}^{-i\theta} - \mathrm{e}^{-2i\theta}) \\ &\quad + \alpha_4(\mathrm{e}^{2i\theta} - 4\mathrm{e}^{i\theta} + 6 - 4\mathrm{e}^{-i\theta} + \mathrm{e}^{-2i\theta}) \\ &\quad + \gamma(\mathrm{e}^{2i\theta} - 5\mathrm{e}^{i\theta} + 10 - 10\mathrm{e}^{-i\theta} + 5\mathrm{e}^{-2i\theta} - \mathrm{e}^{-3i\theta}),\end{aligned}$$

where $\alpha_1 = \nu/2$, $\gamma = 0$ for the quartic and $\gamma = \alpha_5$ for the quintic.
We can write, $\kappa(\theta) = \mathbf{R}(\theta) + i\mathbf{I}(\theta)$, where

$$\begin{aligned}\mathbf{R}(\theta) &= 1 - 2\alpha_2(1-\cos\theta) - 2\alpha_3(\cos\theta - 1)^2 + 4\alpha_4(\cos\theta - 1)^2 \\ &+ \gamma(4(1-\cos^4\theta) + 15\cos\theta(\cos\theta - 1))\end{aligned}$$

$$\mathbf{I}(\theta) = 2\alpha_1 \sin\theta + \alpha_3(2\sin\theta(\cos\theta - 1) - \sin\theta) + \gamma(4\sin\theta(\cos\theta-1)^2 + \sin\theta)$$

For $\theta = \pi$, we have $\mathbf{I}(\pi) = 0$ and $\mathbf{R}(\pi) = 1 - 4\alpha_2 - 8\alpha_3 + 16\alpha_4 + 30\gamma$.
If the schemes are stable then $|\kappa(\pi)| \leq 1$, that is

$$2\alpha_2 + 4\alpha_3 - 8\alpha_4 - 15\gamma \geq 0, \quad 2\alpha_2 + 4\alpha_3 - 8\alpha_4 - 15\gamma \leq 1.$$

(a) For the quartic we have $\gamma = 0$ and then

$$2\alpha_2 + 4\alpha_3 - 8\alpha_4 \geq 0, \quad 2\alpha_2 + 4\alpha_3 - 8\alpha_4 \leq 1.$$

(b) For the quintic we have $0 \leq 2\alpha_2 + 4\alpha_3 - 8\alpha_4 - 15\alpha_5 \leq 1$. □

Although, we have obtained only necessary analytical stability conditions for the quartic and quintic schemes, in Figure 2, we plot necessary and sufficient conditions computed numerically. We observe from these calculations that for the quartic scheme, the conditions

$$0 \leq 2\alpha_2 + 4\alpha_3 - 8\alpha_4 \leq 1$$

are necessary and sufficient for stability.

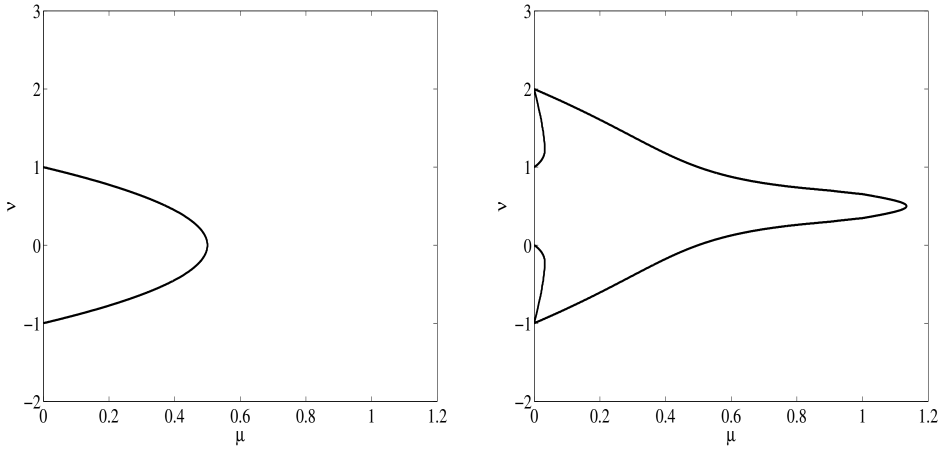

FIGURE 1. Fourier stability region for: (a) Quadratic (b) Cubic

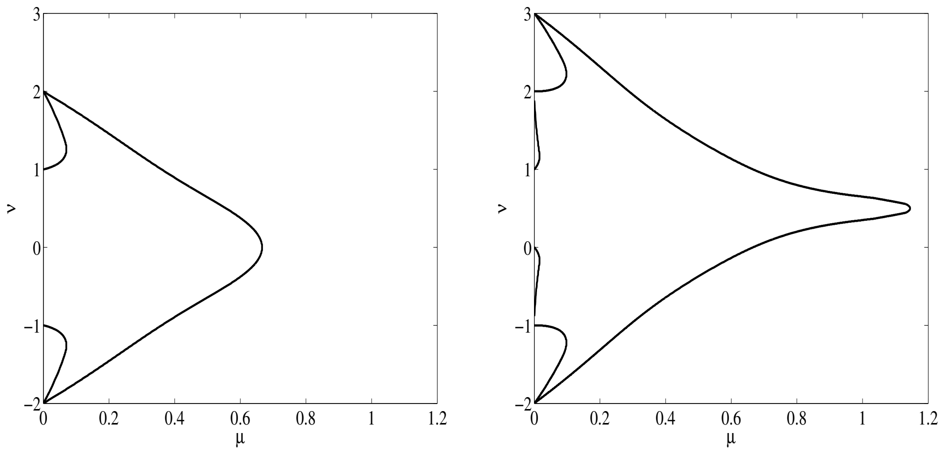

FIGURE 2. Fourier stability region for: (a) Quartic (b) Quintic

2.4. Test problem: periodic boundary conditions. Consider the convection-diffusion problem (1)-(2), for $x \in [0, 1]$ and the initial condition $f(x)$ given by

$$f(x) = e^{-(x-0.5)^2/L^2}, \ x \in [0, 1]. \tag{20}$$

The exact solution of this problem can be obtained from the eigenfunctions of the spatial differential operator which are sines and cosines. Hence, the solution is given by means of a Fourier expansion

$$u(x, t) = \sum_{k=-\infty}^{+\infty} b_k e^{-4\pi^2 k^2 D t} e^{2\pi k (x - V t) i}, \tag{21}$$

with

$$b_k = \int_0^1 e^{-(x-0.5)^2/L^2} e^{2\pi k x i} dx.$$

Since we are assuming that the boundary conditions are periodic, the stability region for the numerical methods considered are given by the von Neumann stability analysis studied in the previous section and stated in Figures 1-2.

In Figure 3 we display the exact solution (21) for $L = 0.05$ and different instants of time $t = 0,\ 0.4,\ 0.8$.

Numerical experiments were conducted for different values of V and D and consequently different Courant numbers ν and Péclet numbers **Pe**,

$$\nu = \frac{V\Delta t}{\Delta x}, \qquad \mathbf{Pe} = \frac{V\Delta x}{D}.$$

We display in Table 1 and Table 2 the global error results for small values of the diffusive parameter D, $D = 0.0001$ and $D = 0.000001$. The rate of convergence increases from the cubic scheme to the quintic scheme, according to the fact that the schemes are generated by increasing the degree of interpolation.

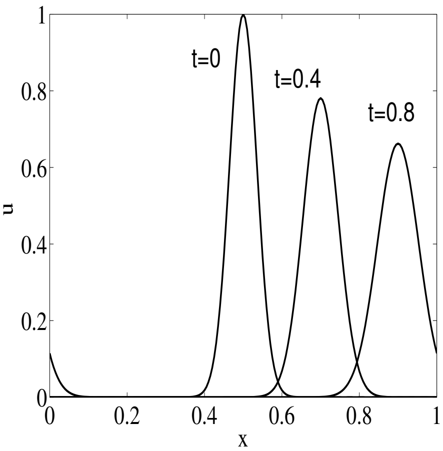

FIGURE 3. Exact solution for t=0, 0.4, 0.8; L=0.05, V=0.5, D=0.001

Schemes	$\Delta x = 0.01$ ($\mu = 0.01$)	$\Delta x = 0.001$ ($\mu = 0.1$)	Convergence rate
cubic	0.19531×10^{-2}	0.26399×10^{-4}	1.87
quartic	0.10578×10^{-2}	0.14908×10^{-5}	2.85
quintic	0.87713×10^{-4}	0.12417×10^{-7}	3.85

Table 1. Global L_2 error of time converged solution for two mesh resolutions at $t = 0.8$ for $\nu = 1$, $V = 1$, $D = 0.0001$. **Pe**$=1000\Delta x$

Schemes	$\Delta x = 0.01$ ($\mu = 0.00001$)	$\Delta x = 0.001$ ($\mu = 0.0001$)	Convergence rate
cubic	0.26944×10^{-4}	0.85748×10^{-6}	1.50
quartic	0.15432×10^{-4}	0.53192×10^{-7}	2.48
quintic	0.13799×10^{-5}	0.49726×10^{-9}	3.44

Table 2. Global L_2 error of time converged solution for two mesh resolutions at $t = 0.8$ for $\nu = 1$, $V = 1$, $D = 0.000001$. **Pe**=$100000\Delta x$

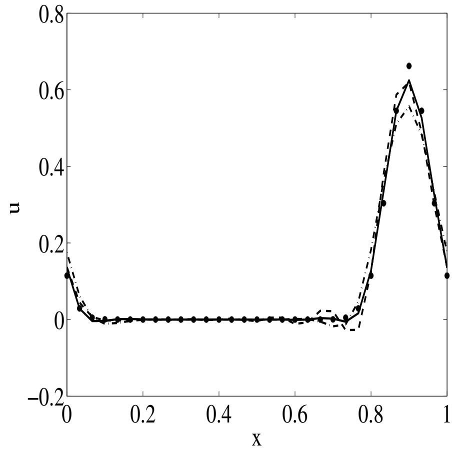

FIGURE 4. Solutions for t=0.8, V=0.5, D=0.001. Exact •; Numerical solutions: cubic (−·), quartic (−−), quintic (−); $\nu = 0.1$; $\Delta x = 0.03$ ($N = 30$, N number of nodes)

In Tables 3 and 4 the diffusive parameter D is closer to the convective parameter V and we consider two different Courant numbers, $\nu = 0.01$ in Table 3 and $\nu = 0.1$ in Table 4. The order of accuracy improves in all methods comparatively to the examples in Table 1 and 2. Additionally, we observe that the order of accuracy improves as the Courant number increases. Furthermore, the cubic and quartic methods evidences dispersive oscillations that are less present in the quintic scheme (see Figure 4). These oscillations diminishes as the Courant number increases and completely disappear around $\nu = 0.8$.

Schemes	$\Delta x = 0.01$ ($\mu = 0.002$)	$\Delta x = 0.001$ ($\mu = 0.02$)	Convergence rate
cubic	0.16248×10^{-1}	0.59929×10^{-4}	2.43
quartic	0.33158×10^{-2}	0.92258×10^{-6}	3.56
quintic	0.61252×10^{-3}	0.68233×10^{-8}	4.95

Table 3. Global L_2 error of time converged solution for two mesh resolutions at $t = 0.8$ for $\nu = 0.01$, $V = 0.5$, $D = 0.001$. **Pe**=$500\Delta x$

Schemes	$\Delta x = 0.01$ ($\mu = 0.02$)	$\Delta x = 0.001$ ($\mu = 0.2$)	Convergence rate
cubic	0.136805×10^{-1}	0.176549×10^{-4}	2.88
quartic	0.285106×10^{-2}	0.105165×10^{-6}	4.43
quintic	0.511304×10^{-3}	0.694070×10^{-9}	5.86

Table 4. Global L_2 error of time converged solution for two mesh resolutions at $t = 0.8$ for $\nu = 0.1$, $V = 0.5$, $D = 0.001$. **Pe**$=500\Delta x$

The cases where the diffusive parameter D is more dominant are shown in Tables 5 and 6. The order of accuracy of the cubic and quintic seems to decrease considerably, specially in Table 6, where the convective parameter is even smaller than in Table 5. The quartic in these cases seems to be a good option. Note that in Table 6 the Courant number was choosen to be $\nu = 0.005$ in order that we can run all schemes inside their stability regions.

Schemes	$\Delta x = 0.01$ ($\mu = 0.02$)	$\Delta x = 0.001$ ($\mu = 0.2$)	Convergence rate
cubic	0.33183×10^{-3}	0.44909×10^{-5}	1.87
quartic	0.21144×10^{-4}	0.76775×10^{-9}	4.44
quintic	0.65020×10^{-6}	0.84342×10^{-10}	3.89

Table 5. Global L_2 error of time converged solution for two mesh resolutions at $t = 0.8$ for $\nu = 0.01$, $V = 0.5$, $D = 0.01$. **Pe**$=50\Delta x$

Schemes	$\Delta x = 0.01$ ($\mu = 0.05$)	$\Delta x = 0.001$ ($\mu = 0.5$)	Convergence rate
cubic	0.47138×10^{-4}	0.46721×10^{-5}	1.00
quartic	0.37026×10^{-6}	0.17707×10^{-9}	3.32
quintic	0.16133×10^{-6}	0.89163×10^{-10}	3.23

Table 6. Global L_2 error of time converged solution for two mesh resolutions at $t = 0.8$ for $\nu = 0.005$, $V = 0.1$, $D = 0.01$. **Pe**$=10\Delta x$

In conclusion, the quartic is a good option for the cases where the convective parameter is less dominant, that is, small Péclet numbers and the quintic is by far the best option for big Péclet numbers. These includes small values of D, which is the case the convection-diffusion equation approaches the non-diffusive hyperbolic equation.

3. In the presence of an inflow boundary condition

Consider the initial boundary condition problem with the convection-diffusion equation (1) defined on the half-line, $x > 0$, with the initial condition

$$u(x, 0) = f(x), \quad x > 0 \tag{22}$$

and the boundary conditions

$$u(0,t) = g(t), \quad t > 0 \quad u(x,t) \to 0, \quad x \to \infty. \tag{23}$$

We are going to apply the high-order schemes studied earlier to this problem. Therefore we need to consider numerical boundary conditions. In this section we study which numerical boundary conditions are more adequate for the quartic and the quintic approximations.

3.1. Numerical boundary conditions. For the quintic approximation we need to consider numerical boundaries at the first two nodes, $j = 1$ and $j = 2$.

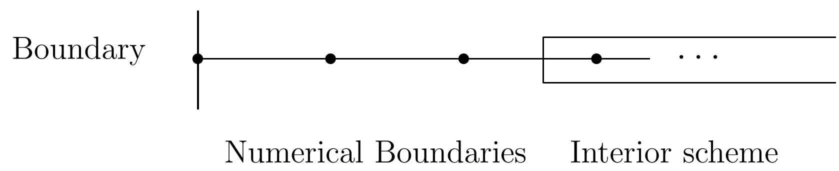

The first idea is to preserve the same degree of interpolation. We derive numerical boundary conditions at $j = 1$ and $j = 2$ as follows: for $j = 1$ we interpolate the mesh points $U_{j-1}, \ldots, U_{j+4}$ and for $j = 2$ we interpolate the mesh points $U_{j-2}, \ldots, U_{j+3}$.

For $j = 1$ we get

$$\begin{aligned} U_j^{n+1} \;=\; & \{1 - \nu\Delta_0 + \frac{1}{2}(\nu^2 + 2\mu)\delta^2 + \frac{1}{6}\nu(1 - \nu^2 - 6\mu)\delta^2\Delta_+ \\ & + \frac{1}{24}[-(\nu^2 + 2\mu) - 2\nu + 2\nu(\nu^2 + 6\mu) + (\nu^4 + 12\nu^2\mu + 12\mu^2)]\delta^2\Delta_+^2 \\ & + \frac{1}{120}[6\nu + 5(\nu^2 + 2\mu) - 5(\nu^3 + 6\nu\mu) - 5(\nu^4 + 12\nu^2\mu + 12\mu^2) \\ & -(\nu^5 + 20\nu^3\mu + 60\nu\mu^2)]\delta^2\Delta_+^3\}U_j^n. \end{aligned} \tag{24}$$

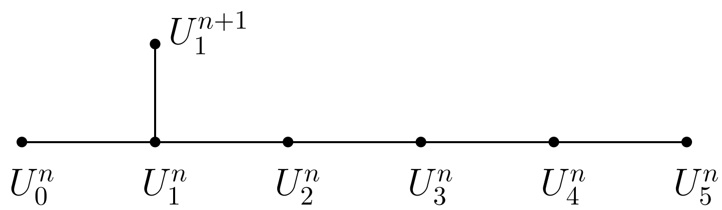

For $j = 2$ we have

$$\begin{aligned} U_j^{n+1} &= \{1 - \nu\Delta_0 + \frac{1}{2}(\nu^2 + 2\mu)\delta^2 + \frac{\nu}{6}(1 - \nu^2 - 6\mu)\delta^2\Delta_- \\ &\quad + \frac{1}{24}[-(\nu^2 + 2\mu) + 2\nu - 2\nu(\nu^2 + 6\mu) + (\nu^4 + 12\nu^2\mu + 12\mu^2)]\delta^4 \\ &\quad + \frac{1}{120}[-4\nu + 5(\nu^3 + 6\nu\mu) - (\nu^5 + 20\nu^3\mu + 60\nu\mu^2)]\delta^2\Delta_-^3\}U_j^n. \quad (25) \end{aligned}$$

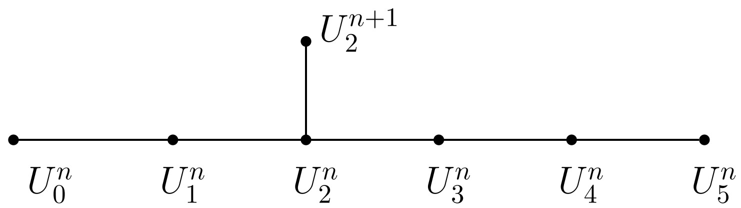

At the first and second nodes, we can also choose lower degrees of interpolation: quadratic, cubic and quartic.

The quadratic interpolation at the first node, $j = 1$, leads to the Lax-Wendroff scheme (7).

A cubic downwind interpolation at $j = 1$, that interpolates the mesh points U_{j-1}^n, U_j^n, U_{j+1}^n and U_{j+2}^n, is given by

$$U_j^{n+1} = \{1 - \nu\Delta_0 + (\frac{1}{2}\nu^2 + \mu)\delta^2 + \frac{1}{6}\nu(1 - \nu^2 - 6\mu)\delta^2\Delta_+\}U_j^n. \quad (26)$$

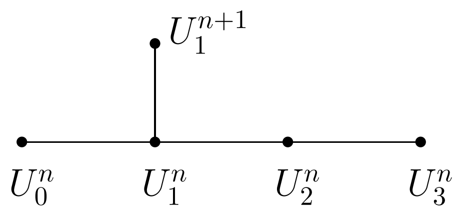

A quartic interpolation at $j = 1$, that interpolates the points U_{j-1}^n, U_j^n, U_{j+1}^n and U_{j+2}^n and U_{j+3}^n, is given by

$$\begin{aligned} U_j^{n+1} &= \{1 - \nu\Delta_- + \frac{1}{2}(\nu^2 + 2\mu - \nu)\delta^2 + \frac{1}{6}\nu(1 - \nu^2 - 6\mu)\delta^2\Delta_+ \\ &\quad + \frac{1}{24}[-(\nu^2 + 2\mu) - 2\nu + 2\nu(\nu^2 + 6\mu) + (\nu^4 + 12\nu^2\mu + 12\mu^2)]\delta^2\Delta_+^2. \quad (27) \end{aligned}$$

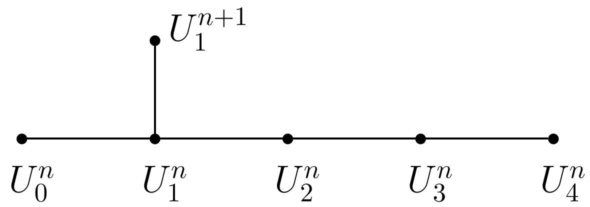

At the second node, $j = 2$, we can consider the quadratic interpolation (7), the cubic interpolation (8) and also the quartic interpolation (9), derived previously.

Let us now describe in detail the schemes we are going to study.

We consider the Quickest scheme (cubic interpolation) with the third-order numerical boundary condition (26) for a self contained study. Note that in [10] it is shown that the Quickest scheme with the third-order numerical boundary condition (26) or with the second-order boundary condition (7) at $j = 1$ gives similar accuracy results.

We proceed as follows. We denote $cubic_3$ the cubic approximation with the numerical boundary condition (26). For the quartic approximation we use the notation

$$quartic_{j_1}, \quad j_1 = 2, 3, 4.$$

The value of j_1 denotes the numerical boundary condition considered at $j = 1$, according to its order of accuracy, that is, $j_1 = 2$ denotes the scheme (7), $j_1 = 3$ denotes the scheme (26) and $j_1 = 4$ denotes the scheme (27).

Similarly, for the quintic approximation we use the notation

$$quintic_{j_1 j_2}, \quad j_1, j_2 = 2, 3, 4, 5.$$

Now, we have an additional numerical boundary condition. The value j_1 still denotes the boundary condition at the first node, $j = 1$, and j_2 denotes the numerical boundary condition at the second node, $j = 2$. For the first node, $j_1 = 2, 3, 4$ denotes the same as in the quartic scheme and $j_1 = 5$ denotes the scheme (24). For the second node, $j_2 = 2$ denotes the scheme (7), $j_2 = 3$ denotes the scheme (8), $j_2 = 4$ denotes the scheme (9) and $j_2 = 5$ denotes the scheme (25).

3.2. Global error and stability analysis. The numerical schemes studied, with the numerical boundary conditions presented, can still be written in the matricial form (11), although the matrix A is now different, taking into account the numerical boundary conditions. Furthermore, we still have the global error given by (12).

In this section, it is very likely that A is a non-normal matrix and therefore the condition $||A|| \leq 1$, is not anymore an adequate stability condition as in section 2.2.

We have

$$E^{n+1} = A^{n+1}E^0 + \Delta t \sum_{j=0}^{n} A^j T^{n-j}.$$

Then a global error bound is given by

$$||E^{n+1}|| \leq ||A^{n+1}|| ||E^0|| + (n+1)\Delta t \max_{0\leq j\leq n} ||A^j|| ||T^{n-j}||.$$

Furthermore, if $||A||$ is a matrix such that $||A^n|| \leq K$, for $0 < n\Delta t \leq T$, then we say that we have Lax stability and

$$||E^n|| \leq K||E^0|| + n\Delta t K||T^{n-1-j}||.$$

For A non-normal, there is usually a transient behaviour of powers before they start to decay exponentially.

For our methods if $\rho(A) > 1$ the scheme is unstable. We plot the regions where the schemes are unstable Figure 5 – 7. Note that outside the von Neumann stability region, shown in Figures 1-2, for the interior scheme, the numerical methods with the numerical boundary conditions are still unstable. Therefore, the small part, on the top left of Figures 5 – 7, that is, for small μ and $\nu \geq 1$, is unstable according to the von Neumann analysis.

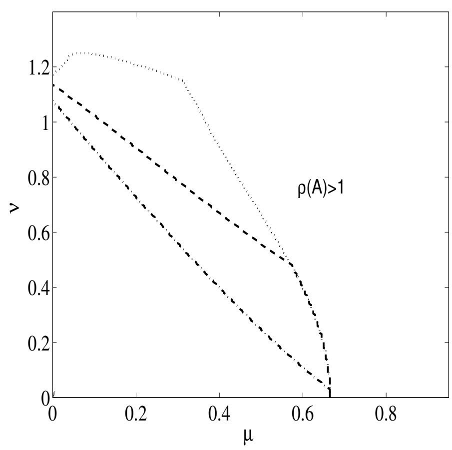

FIGURE 5. Quartic approximation with different numerical boundary conditions: quartic$_4$ $(- \cdot -)$; quartic$_3$ $(--)$;quartic$_2$ $(\cdots)$

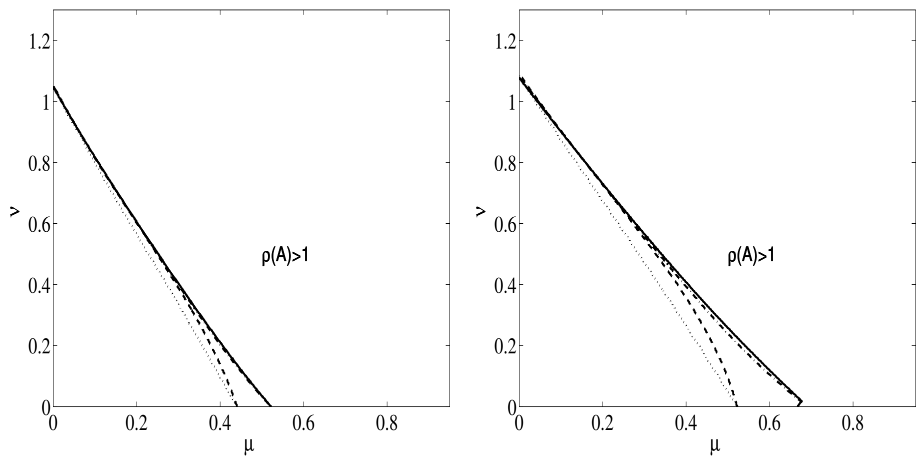

FIGURE 6. Quintic approximation with different numerical boundary conditions: (a) quintic$_{55}$ (−); quintic$_{54}$ (− · −); quintic$_{53}$ (−−);quintic$_{52}$ (· · ·). (b) quintic$_{45}$ (−); quintic$_{44}$ (− · −); quintic$_{43}$ (−−);quintic$_{42}$ (· · ·).

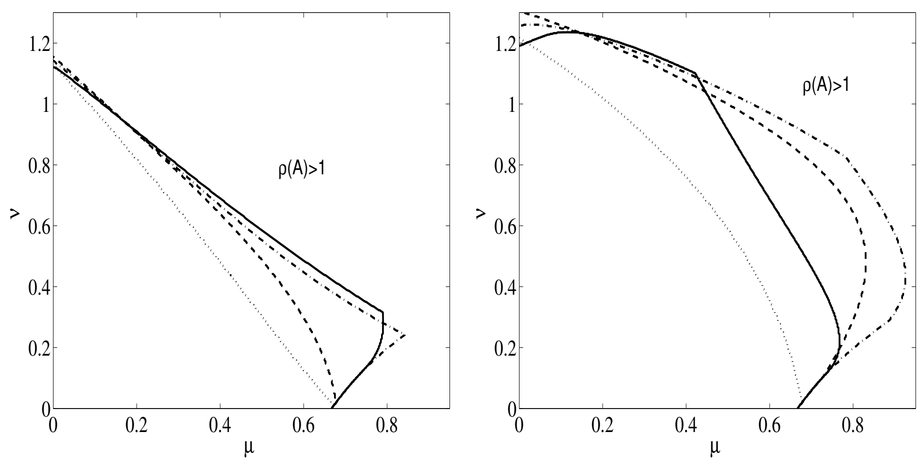

FIGURE 7. Quintic approximation with different numerical boundary conditions: (a) quintic$_{35}$ (−); quintic$_{34}$ (− · −); quintic$_{33}$ (−−);quintic$_{32}$ (· · ·).(b) quintic$_{25}$ (−); quintic$_{24}$ (− · −); quintic$_{23}$ (−−);quintic$_{22}$ (· · ·).

3.3. Test problem: an inflow boundary condition. If we consider the convection-diffusion problem (1), (22) and (23), then an exact solution of this system on the half line $x \geq 0$ is given by

$$\begin{aligned} u(x,t) &= \frac{1}{\sqrt{\pi}}\int_0^t g(t-\tau)G^*(x,\tau)d\tau \\ &\quad +\frac{1}{\sqrt{\pi}}\int_{\frac{Vt-x}{2\sqrt{Dt}}}^{+\infty} f(x-Vt+2\sqrt{Dt}\xi)\mathrm{e}^{-\xi^2}d\xi \end{aligned}$$

$$-\frac{1}{\sqrt{\pi}}\int_{\frac{Vt+x}{2\sqrt{Dt}}}^{+\infty} f(-x-Vt+2\sqrt{Dt}\xi)\mathrm{e}^{Vx/D}\mathrm{e}^{-\xi^2}d\xi \qquad (28)$$

where the function $G^*(x,\tau)$ is given by

$$G^*(x,\tau) = \frac{x}{2\sqrt{D}\tau^{2/3}}\mathrm{e}^{-(x-V\tau)^2/4D\tau}.$$

Consider the initial data

$$u(x,0) = \mathrm{e}^{-x^2}, \quad x > 0, \quad u(0,t) = 0, \quad t \geq 0.$$

Our reason for considering this test case is that it is straightforward to calculate an exact solution for this initial profile:

$$\begin{aligned} u(x,t) \;&=\; \frac{1}{2\sqrt{4Dt+1}}\left[\mathrm{e}^{-\dfrac{(x-Vt)^2}{4Dt+1}}\mathrm{Erfc}\left(-\frac{(x-Vt)}{2\sqrt{Dt(4Dt+1)}}\right)\right. \\ &\qquad \left. -\mathrm{e}^{-\dfrac{(x+Vt)^2}{4Dt+1}+\dfrac{Vx}{D}}\mathrm{Erfc}\left(\frac{(x+Vt)}{2\sqrt{Dt(4Dt+1)}}\right)\right], \end{aligned} \qquad (29)$$

where $\mathrm{Erfc}(x) = \dfrac{2}{\sqrt{\pi}}\displaystyle\int_x^{\infty}\mathrm{e}^{-s^2}\mathrm{d}s$. The time evolution of the solution is shown in Figure 8, at the times $t = 0, 5, 10, 20$ and for $V = 0.5$ and $D = 0.001$.

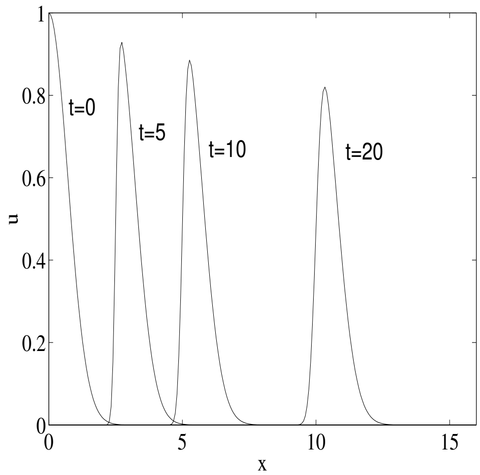

FIGURE 8. Exact solution defined by (29) at the times t=0, 5, 10, 20, for $V = 0.5$ and $D = 0.001$.

In what follows, for the initial solution $u(x,0) = \mathrm{e}^{-x^2}$, we compute the approximate solutions for a finite domain $0 \leq x \leq 6$ at $t = 5$.

Table 7 and Table 8 show the global L_2 error for the cubic, quartic and quintic with different numerical boundary conditions. In Table 7, we assume $V = 0.5,\ D = 0.001$ and in Table 8 $V = 0.5,\ D = 0.0001$. The convergence in the second case is slower, that is, for the same space step, the error is smaller for $D = 0.001$ (Table 7) than for $D = 0.0001$ (Table 8). In the later case we have a steepest gradient, as we can see in Figure 10, and therefore to remove the oscillations is more difficult. Also the differences between Table 7 and Table 8 confirms what was observed for the periodic case: the quintic approximation shows to be considerably advantageous over the quartic scheme for small values of D.

For the quartic, all the numerical boundary conditions chosen seems to give good results. Note that the $quartic_2$ performs quite well.

Schemes		Error L_2			Convergence
		$\Delta x = 0.1$	$\Delta x = 0.05$	$\Delta x = 0.01$	p
cubic	$cubic_3$	0.2402E-00	0.1177E-00	0.3802E-02	1.80
$quartic$	$quartic_4$	0.2768E-00	0.7074E-01	0.8088E-03	2.53
	$quartic_3$	0.2529E-00	0.7733E-01	0.8099E-03	2.49
	$quartic_2$	0.2317E-00	0.7978E-01	0.8026E-03	2.46
$quintic_{5n}$	$quintic_{55}$	0.2825E-00	0.2690E-01	0.8415E-03	2.53
	$quintic_{54}$	0.1174E-00	0.2195E-01	0.8417E-03	2.14
	$quintic_{53}$	0.1276E-00	0.2860E-01	0.8386E-03	2.18
	$quintic_{52}$	0.3817E-00	0.9638E-01	0.1091E-02	2.54
$quintic_{4n}$	$quintic_{45}$	0.1506E-00	0.1956E-01	0.8429E-03	2.25
	$quintic_{44}$	0.1279E-00	0.2089E-01	0.8430E-03	2.18
	$quintic_{43}$	0.1283E-00	0.2687E-01	0.8407E-03	2.18
	$quintic_{42}$	0.3134E-00	0.7683E-01	0.9384E-03	2.52
$quintic_{3n}$	$quintic_{35}$	0.1331E-00	0.2425E-01	0.8378E-03	2.20
	$quintic_{34}$	0.1396E-00	0.2638E-01	0.8378E-03	2.22
	$quintic_{33}$	0.1407E-00	0.3021E-01	0.8367E-03	2.23
	$quintic_{32}$	0.2396E-00	0.6033E-01	0.8034E-03	2.47
$quintic_{2n}$	$quintic_{25}$	0.1474E-00	0.3870E-01	0.6957E-03	2.33
	$quintic_{24}$	0.1531E-00	0.4007E-01	0.6946E-03	2.34
	$quintic_{23}$	0.1580E-00	0.4270E-01	0.6939E-03	2.36
	$quintic_{22}$	0.1927E-00	0.5496E-01	0.6906E-03	2.45

Table 7. Global L_2 error of time converged solution for three mesh resolutions: $t = 5$, $x \in [0,6]$, $D = 0.001$, $V = 0.5$, $\nu = 0.01$
Convergence rate p: between $\Delta x = 0.1$ and $\Delta x = 0.01$;

Concerning the quintic, if we take into account both cases, $D = 0.001$ (Table 7) and $D = 0.0001$ (Table 8), the best results seems to be given by $quintic_{54}$, $quintic_{44}$ (although similar to $quintic_{45}$), and $quintic_{35}$ (although similar to $quintic_{34}$).

In Figures 9-10 we plot results for the $cubic_3$, $quartic_4$, $quintic_{54}$ and $quintic_{35}$. The quintic presents smaller oscillations and they disappear more quickly as we refine the mesh.

Schemes		Error L_2			Convergence
		$\Delta x = 0.05$	$\Delta x = 0.025$	$\Delta x = 0.005$	p
cubic	$cubic_3$	0.4225E-00	0.3222E-00	0.3845E-01	1.04
quartic	$quartic_4$	0.5304E-00	0.3160E-00	0.5252E-02	2.00
	$quartic_3$	0.4741E-00	0.3121E-00	0.5376E-02	1.95
	$quartic_2$	0.4348E-00	0.2955E-00	0.6430E-02	1.83
$quintic_{5n}$	$quintic_{55}$	0.6185E-00	0.2728E-00	0.1373E-02	2.65
	$quintic_{54}$	0.2524E-00	0.1289E-00	0.1360E-02	2.27
	$quintic_{53}$	0.2708E-00	0.1397E-00	0.1298E-02	2.32
	$quintic_{52}$	0.5027E-00	0.2429E-00	0.3330E-02	2.18
$quintic_{4n}$	$quintic_{45}$	0.2566E-00	0.1249E-00	0.1360E-02	2.28
	$quintic_{44}$	0.2589E-00	0.1277E-00	0.1350E-02	2.28
	$quintic_{43}$	0.2699E-00	0.1376E-00	0.1307E-02	2.31
	$quintic_{42}$	0.4298E-00	0.2071E-00	0.2401E-02	2.25
$quintic_{3n}$	$quintic_{35}$	0.2672E-00	0.1328E-00	0.1246E-02	2.33
	$quintic_{34}$	0.2743E-00	0.1358E-00	0.1241E-02	2.34
	$quintic_{33}$	0.2791E-00	0.1420E-00	0.1236E-02	2.35
	$quintic_{32}$	0.3606E-00	0.1809E-00	0.1472E-02	2.39
$quintic_{2n}$	$quintic_{25}$	0.2857E-00	0.1512E-00	0.1648E-02	2.24
	$quintic_{24}$	0.2901E-00	0.1532E-00	0.1650E-02	2.25
	$quintic_{23}$	0.2942E-00	0.1567E-00	0.1702E-02	2.24
	$quintic_{22}$	0.2280E-00	0.1724E-00	0.1964E-02	2.06

Table 8. Global L_2 error of time converged solution for three mesh resolutions: $t = 5$, $x \in [0, 6]$, $D = 0.0001$, $V = 0.5$, $\nu = 0.01$
Convergence rate p: between $\Delta x = 0.05$ and $\Delta x = 0.005$

We observe that in Table 7 the quintic with second order boundary condition at the first node becomes quite good as we refine the mesh, although this is not an advantage when using high-order schemes, since the main advantage of considering an higher order scheme is to get more accuracy with less refined meshes.

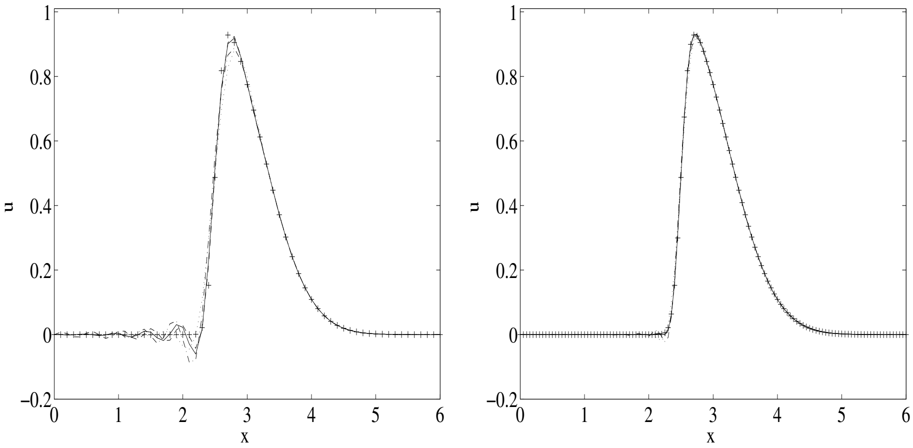

FIGURE 9. Solutions for $V = 0.5$ and $D = 0.001$. Exact solution $(+++)$; cubic$_3$ $(\cdots)$; quartic$_2$ $(-\cdot-)$;quintic$_{54}$ $(--)$; quintic$_{35}$ $(-)$. (a) $\Delta x = 0.1$; (b) $\Delta x = 0.05$

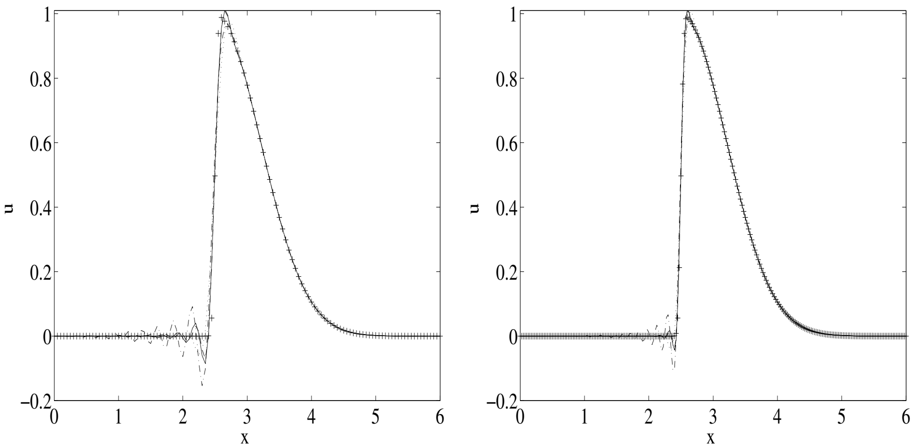

FIGURE 10. Solutions for $V = 0.5$ and $D = 0.0001$. Exact solution $(+++)$; cubic$_3$ $(\cdots)$; quartic$_2$ $(-\cdot-)$;quintic$_{54}$ $(--)$; quintic$_{35}$ $(-)$. (a) $\Delta x = 0.05$; (b) $\Delta x = 0.025$

4. Conclusion

Schemes of high-order have been developed for the discretisation of the convection-diffusion equation. Firstly, we have derived the schemes for an infinite space domain and have analysed its stability and numerical performance for different values of the convective parameter V and the diffusive parameter D and therefore different Courant numbers and Péclet numbers. The quintic scheme seems to be good in general and, comparatively to the quartic scheme, its best performance is for large Péclet numbers.

The second part of the paper is devoted to the presence of an inflow boundary. Implementation of boundary conditions can be problematic with such higher order schemes. Therefore, we present a number of numerical boundary conditions that can be used. According to the numerical results, it seems the quartic scheme performs reasonable well with the numerical boundary conditions of order $O(\Delta x^2)$, $O(\Delta x^3)$ and $O(\Delta x^4)$. For the quintic at the first node, next to the boundary, we can choose a numerical scheme of order at least $O(\Delta x^3)$ and at the second node we are advised to choose an order not less than $O(\Delta x^4)$.

This lead us to conjecture that if we have a scheme of higher order, that is, $O(\Delta x^n)$, we are advised to choose at the first node, next to the boundary, a scheme of order at least $O(\Delta x^{n-2})$ and on the second node a scheme of order at least $O(\Delta x^{n-1})$.

References

[1] Smith, G.D. (1985). *Numerical solution of partial differential equations: finite difference methods*, Oxford University Press: Oxford.

[2] Kolesnikov, A. and Baker, A.J. (2000). Efficient implementation of high order methods for the advection-diffusion equation.

[3] Morton, K.W and I.J Sobey (1993). Discretization of a convection-diffusion equation. *IMA Journal of Numerical Analysis* **13**, 141-160.

[4] Xu, H.Y., M.D. Matovic and A. Pollard (1997). Finite difference schemes for three-dimensional time-dependent convection-diffusion equation using full global discretization. *Journal of Computational Physics* **130**, 109-122.

[5] Lax, P.D. and B. Wendroff (1964). Difference schemes for hyperbolic equations with high order of accuracy. *Communications on Pure and Applied Mathematics* **17**, 381-398.

[6] Leonard, B.P. (1979). A stable and accurate convective modelling procedure based on quadratic upstream interpolation. *Computer Methods in Applied Mechanics and Engineering* **19**, 59-98.

[7] Sod, G.A. (1988). *Numerical methods in fluid dynamics: initial and initial boundary-value problems*, Cambridge University Press: Cambridge.

[8] Warming, F.F. and B.J. Hyett (1974). The modified equation approach to the stability and accuracy analysis of finite difference methods. *Journal of Computational Physics* **14**, 159-179.

[9] Richtmyer, R.D. and K.W. Morton (1967). *Difference methods for initial-value problems.* Wiley-Interscience: New York.

[10] Sousa, E. and Sobey, I.J. (2002) On the influence of numerical boundary conditions *Applied Numerical Mathematics*, **41**, 325-344.

Ercília Sousa
Departamento de Matemática, Universidade de Coimbra, Portugal